Rance, M., Sørensen, O. W., Bodenhausen, G., Wagner, G., Ernst, R. R., & Wüthrich, K. (1983) *Biochem. Biophys. Res. Commun. 117*, 479–485.
Rance, M., Wright, P. E., Messerle, B. A., & Field, L. D. (1987) *J. Am. Chem. Soc. 109*, 1591–1593.
Reid, B. R. (1987) *Q. Rev. Biophys. 20*, 1–34.
Searle, M. S., & Embrey, K. J. (1990) *Nucleic Acids Res. 18*, 3753–3762.
Shaka, A. J., Keeler, J., Frenkiel, T., & Freeman, R. (1983) *J. Magn. Reson. 52*, 335–338.
Sutherland, I. O. (1971) *Annu. Rep. NMR Spectrosc. 4*, 71–225.
Teng, M.-K., Usman, N., Frederick, C. A., & Wang, A. H.-J. (1988) *Nucleic Acids Res. 16*, 2671–2690.
van de Ven, F. J. M., & Hilbers, C. W. (1988) *Eur. J. Biochem. 178*, 1–38.
Wemmer, D. E., & Reid, B. R. (1985) *Annu. Rev. Phys. Chem. 36*, 105–137.
Widmer, H., & Wüthrich, K. (1986) *J. Magn. Reson. 70*, 270–279.
Wüthrich, K. (1986) *NMR of Proteins and Nucleic Acids*, Wiley, New York.
Zimmer, C., & Wähnert, U. (1986) *Prog. Biophys. Mol. Biol. 39*, 31–112.

Assignment of the Aliphatic ^1H and ^{13}C Resonances of the *Bacillus subtilis* Glucose Permease IIA Domain Using Double- and Triple-Resonance Heteronuclear Three-Dimensional NMR Spectroscopy†

Wayne J. Fairbrother,‡,§ Arthur G. Palmer, III,‡,∥ Mark Rance,‡ Jonathan Reizer,⊥ Milton H. Saier, Jr.,⊥ and Peter E. Wright*,‡

Department of Molecular Biology, The Scripps Research Institute, La Jolla, California 92037, and Department of Biology, University of California at San Diego, La Jolla, California 92093-0116

Received December 26, 1991; Revised Manuscript Received February 27, 1992

ABSTRACT: Nearly complete assignment of the aliphatic ^1H and ^{13}C resonances of the IIA^{glc} domain of *Bacillus subtilis* has been achieved using a combination of double- and triple-resonance three-dimensional (3D) NMR experiments. A constant-time 3D triple-resonance HCA(CO)N experiment, which correlates the $^1H^\alpha$ and $^{13}C^\alpha$ chemical shifts of one residue with the amide ^{15}N chemical shift of the following residue, was used to obtain sequence-specific assignments of the $^{13}C^\alpha$ resonances. The $^1H^\alpha$ and amide ^{15}N chemical shifts had been sequentially assigned previously using principally 3D ^1H–^{15}N NOESY-HMQC and TOCSY-HMQC experiments [Fairbrother, W. J., Cavanagh, J., Dyson, H. J., Palmer, A. G., III, Sutrina, S. L., Reizer, J., Saier, M. H., Jr., & Wright, P. E. (1991) *Biochemistry 30*, 6896–6907]. The side-chain spin systems were identified using 3D HCCH-COSY and HCCH-TOCSY spectra and were assigned sequentially on the basis of their $^1H^\alpha$ and $^{13}C^\alpha$ chemical shifts. The 3D HCCH and HCA(CO)N experiments rely on large heteronuclear one-bond J couplings for coherence transfers and therefore offer a considerable advantage over conventional ^1H–^1H correlation experiments that rely on ^1H–^1H ^3J couplings, which, for proteins the size of IIA^{glc} (17.4 kDa), may be significantly smaller than the ^1H line widths. The assignments reported herein are essential for the determination of the high-resolution solution structure of the IIA^{glc} domain of *B. subtilis* using 3D and 4D heteronuclear edited NOESY experiments; these assignments have been used to analyze 3D ^1H–^{15}N NOESY-HMQC and ^1H–^{13}C NOESY-HSQC spectra and calculate a low-resolution structure [Fairbrother, W. J., Gippert, G. P., Reizer, J., Saier, M. H., Jr., & Wright, P. E. (1992) *FEBS Lett. 296*, 148–152].

Glucose-specific enzyme IIA (IIA^{glc}; previously referred to as III^{glc})[1] is the central regulatory protein of the bacterial phosphoenolpyruvate/sugar phosphotransferase system (PTS). Transcriptional regulation by the PTS involves both catabolite repression and inducer exclusion [see Reizer et al. (1988), Saier (1989), and Meadow et al. (1990) for reviews]. In catabolite repression, the phosphorylated form of IIA^{glc} acts as an allosteric activator of adenylate cyclase; in inducer exclusion, the free (unphosphorylated) form functions as an allosteric

† This work was supported by grants from the National Institutes of Heatlh, GM-36643 (P.E.W.), RI-21702 (M.H.S.), and RI-14176 (M. H.S.), and from the National Science Foundation, DMB8903777 (M.R.). W.J.F. was supported by Damon Runyon–Walter Winchell Cancer Research Fund Fellowship DRG-1059. A.G.P. was supported by a National Science Foundation Postdoctoral Fellowship in Chemistry, under Grant CHE-8907510 awarded in 1989.

* To whom correspondence should be addressed.
‡ The Scripps Research Institute.
§ Present address: Genentech, Inc., 460 Point San Bruno Blvd., South San Francisco, CA 94080.
∥ Present address: Department of Biochemistry and Molecular Biophysics, College of Physicians and Surgeons, Columbia University, 630 West 168th St., New York, NY 10032.
⊥ University of California, San Diego.

[1] Abbreviations: 3D, three dimensional; HCA(CO)N, 3D triple-resonance $^1H^\alpha$–$^{13}C^\alpha$–^{15}N correlation spectroscopy; HCCH-COSY, 3D ^1H–^{13}C–^{13}C–^1H correlation spectroscopy via $^1J_{CC}$ couplings; HCCH-TOCSY, 3D ^1H–^{13}C–^{13}C–^1H total correlation spectroscopy via isotropic mixing of ^{13}C magnetization; ^1H–^{13}C NOESY-HMQC, 3D heteronuclear ^1H nuclear Overhauser ^1H–^{13}C multiple-quantum coherence spectroscopy; ^1H–^{13}C NOESY-HSQC, 3D heteronuclear ^1H nuclear Overhauser ^1H–^{13}C single-quantum coherence spectroscopy; HNCA, 3D triple-resonance NH–^{15}N–$^{13}C^\alpha$ correlation spectroscopy; ^1H–^{15}N NOESY-HMQC, 3D heteronuclear ^1H nuclear Overhauser ^1H–^{15}N multiple-quantum coherence spectroscopy; ^1H–^{15}N TOCSY-HMQC, 3D heteronuclear ^1H total correlation ^1H–^{15}N multiple-quantum coherence spectroscopy; IIA^{glc}, glucose specific enzyme IIA; NMR, nuclear magnetic resonance; NOE, nuclear Overhauser effect; PTS, phosphoenolpyruvate/sugar phosphotransferase system; rf, radiofrequency; TMS, tetramethylsilane; TPPI, time-proportional phase incrementation; TSP, 3-(trimethylsilyl)propionic acid; TSS, 3-(trimethylsilyl)propanesulfonic acid.

0006-2960/92/0431-4413$03.00/0

inhibitor of several permeases and catabolic enzymes that generate endogenous inducers of non-PTS operons. In addition, IIA^{glc} interacts with other PTS proteins, specifically the histidine-containing phosphocarrier protein (HPr) and the membrane bound IIB^{glc}, in the transfer of a phosphoryl group from phosphoenolpyruvate to glucose.

Unlike *Escherichia coli*, which has an autonomous IIA^{glc} protein, *Bacillus subtilis* possesses a glucose permease with a cytosolic C-terminal IIA domain covalently linked, via a flexible Q-linker (Wootton & Drummond, 1989), to the membrane-bound $IICB^{glc}$ domains (Sutrina et al., 1990). The 162-residue IIA^{glc} domain of *B. subtilis* has recently been overexpressed in *E. coli*, where it assumes both the functional and regulatory roles of the soluble *E. coli* enzyme IIA^{glc} protein (Sutrina et al., 1990; Dean et al., 1990; Reizer et al., 1991).

We have recently reported the assignment of the ^1H and ^{15}N backbone resonances and the determination of the secondary structure of the *B. subtilis* IIA^{glc} domain, using primarily three-dimensional (3D) heteronuclear ^1H–^{15}N NMR spectroscopy (Fairbrother et al., 1991). Using these techniques, the aliphatic ^1H resonances of many residues could not be assigned because extensive chemical shift overlap occurs in the aliphatic region of the spectra and coherence transfer in the 3D ^1H–^{15}N TOCSY-HMQC experiment is inefficient for the longer side chains. Such problems are typical for proteins the size of the IIA^{glc} domain and have led to the development of heteronuclear NMR techniques that rely on uniformly large one-bond ^1H–^{13}C, ^{13}C–^{13}C, ^{13}C–^{15}N, and ^1H–^{15}N scalar J coupling constants, rather than on the small and variable ^1H–^1H scalar ^3J coupling constants, to establish through-bond connectivities (Kay et al., 1990a,b; Ikura et al., 1990; Fesik et al., 1990; Bax et al., 1990a,b; Clore et al., 1990).

Here we report the use of such experiments in the assignment of the aliphatic ^1H and ^{13}C resonances of the *B. subtilis* IIA^{glc} domain. Beginning with the previously assigned amide ^{15}N and $^1H^{\alpha}$ resonances (Fairbrother et al., 1991), sequential assignments for the $^{13}C^{\alpha}$ chemical shifts were obtained by using a 3D HCA(CO)N triple-resonance experiment (Kay et al., 1990b; Ikura et al., 1990; Powers et al., 1991; Palmer et al., 1992). Assignment of the side-chain spin systems was completed using 3D HCCH-COSY (Bax et al., 1990a; Clore et al., 1990) and HCCH-TOCSY (Bax et al., 1990b; Clore et al., 1990) experiments. The assignments reported here have enabled analysis of 3D ^1H–^{15}N NOESY-HMQC and ^1H–^{13}C NOESY-HSQC spectra and have led to the determination of a low-resolution solution structure of the IIA^{glc} domain (Fairbrother et al., 1992). An X-ray crystal structure of the IIA^{glc} domain of *B. subtilis* has also recently been published (Liao et al., 1991). The overall folds of the independently determined NMR solution structure and the X-ray crystal structure appear very similar. The ^1H, ^{15}N, and ^{13}C resonance assignments of the homologous *E. coli* IIA^{glc} protein (Pelton et al., 1991a) have been determined using a strategy similar to that applied by Ikura et al. (1990, 1991a) to calmodulin. The secondary structure of *E. coli* IIA^{glc} determined using these assignments to analyze 3D ^1H–^{15}N and ^1H–^{13}C NOESY-HMQC spectra (Pelton et al., 1991b) is similar to that of the IIA domain of the *B. subtilis* glucose permease (Fairbrother et al., 1991). An X-ray crystal structure of the IIA^{glc} protein from *E. coli* has also recently been reported (Worthylake et al., 1991).

Experimental Procedures

Sample Preparation. The overproduction and purification of *B. subtilis* IIA^{glc} domain (hereafter referred to as IIA^{glc}) was as described previously (Sutrina et al., 1990; Reizer et al., 1991). Uniform $^{15}N/^{13}C$ labeling (>95%) was performed by growing the cells in minimal medium containing 0.08% (w/v) $(^{15}NH_4)_2SO_4$ as the sole nitrogen source and 0.2% (w/v) [$^{13}C_6$]glucose as the sole carbon source. NMR samples contained ~2.0 mM IIA^{glc} (10 mM potassium phosphate, pH 6.6, 99.99% D_2O). N-terminal sequencing was performed on an Applied Biosystems 470A gas-phase sequencer.

NMR Measurements. All NMR spectra were recorded at 308 K on a Bruker AMX500 spectrometer, equipped with a three-channel interface. Proton chemical shifts were referenced to internal dioxane (3.75 ppm downfield of TSS). The ^{15}N and ^{13}C chemical shifts were indirectly referenced to liquid NH_3 and TMS, respectively, by multiplying the spectrometer frequency corresponding to 0 ppm in the ^1H spectrum by the $^{15}N/^1H$ frequency ratio (0.1013291444; Live et al., 1984) or by the $^{13}C/^1H$ frequency ratio (0.25145002; Bax & Subramanian, 1986). Note that the ^{13}C chemical shifts referenced to TMS are approximately 1.9 ppm upfield from those referenced to TSP (Bax & Subramanian, 1986). Uncertainties in the reported chemical shifts are 0.02, 0.2, and 0.1 ppm for ^1H, ^{13}C, and ^{15}N, respectively.

The 3D constant-time HCA(CO)N experiment was performed using a new pulse scheme (Palmer et al., 1992) that allows spectra to be acquired with higher resolution in t_1 than was possible in the original schemes (Kay et al., 1990b; Ikura et al., 1990; Powers et al., 1991) and thus eliminates the need for linear prediction of the data in this dimension. The ^1H, aliphatic ^{13}C, and ^{15}N radiofrequency (rf) pulses were generated using the three spectrometer rf channels. Carbonyl ^{13}C pulses were generated using an auxiliary fourth channel as described previously (Palmer et al., 1992). GARP-1 phase modulation was used for ^{13}C decoupling during acquisition (Shaka et al., 1985). The ^1H, aliphatic ^{13}C, carbonyl ^{13}C, and ^{15}N carrier frequencies were set to 4.7, 52.5, 177, and 116 ppm, respectively. Quadrature detection in t_1 and t_2 was achieved using the TPPI-States method (Marion et al., 1989). The t_1, t_2, and t_3 dimensions were digitized with 58 × 32 × 512 complex data points and have spectral widths of 3.33, 1.75, and 12.5 kHz and total acquisition times of 17.4, 18.3, and 41.0 ms, respectively. The ^{13}C rf field strengths were adjusted such that carbonyl nuclei were minimally excited by pulses applied to aliphatic nuclei and vice versa (Palmer et al., 1991). The t_1 and t_2 sampling delays were adjusted to be one-half of the respective increment, resulting in a −180° first-order phase correction being necessary. As a result, peaks which were folded in the F_2 dimension (no peaks were folded in the F_1 dimension) had opposite phase to the unfolded resonances (Bax et al., 1991).

The HCCH-COSY experiment was performed essentially as described by Bax et al. (1990a) except that the carbonyl inversion pulse during the t_2 period was applied on resonance using the third rf channel. The HCCH-TOCSY experiment was also performed as described previously (Bax et al., 1990b) except that the carbonyl inversion pulse was applied on resonance and ^{13}C isotropic mixing was achieved using the DIPSI-2 rather than the DIPSI-3 sequence (Shaka et al., 1988). In both cases, ^{13}C decoupling during acquisition was carried out with GARP-1 phase modulation. For both experiments, the ^1H carrier was placed at 3.0 ppm and the ^{13}C carrier at 41.4 ppm. The ^1H and ^{13}C pulses were applied with 24 and 9.5 kHz rf field strengths, respectively; DIPSI-2 mixing in the HCCH-TOCSY experiment used a 7.7 kHz rf field. For the HCCH-TOCSY experiment, the ^{13}C pulses were generated using an auxiliary amplifier (model 3205, American Microwave Technology) capable of sustaining a >10% duty cycle.

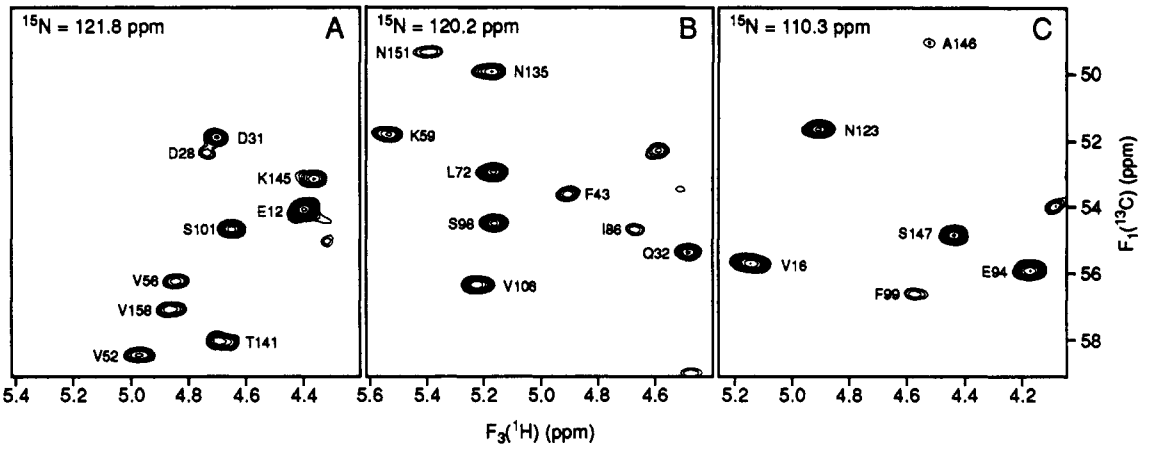

FIGURE 1: Representative $F_2(^{15}N)$ planes from the 3D HCA(CO)N spectrum of uniformly $^{15}N/^{13}C$-labeled IIA^{glc} at ^{15}N chemical shifts of 121.8 (A), 120.2 (B), and 110.3 ppm (C). The cross-peaks are labeled according to the $F_1(^{13}C^{\alpha})$–$F_3(^1H^{\alpha})$ assignments.

The length of the DIPSI-2 isotropic mixing period was 22.5 ms. Quadrature detection in t_1 and t_2 was achieved using the TPPI-States and the States methods, respectively (Marion et al., 1989). The t_1, t_2, and t_3 dimensions were digitized with 128 × 32 × 512 complex data points, have spectral widths of 4.0, 4.5, and 12.5 kHz, and total acquisition times of 32.0, 7.0, and 41.0 ms, respectively. The t_1 sample delays for both experiments and the t_2 sampling delay in the HCCH-TOCSY experiment were adjusted to one-half of the respective increment, which resulted in a need for a −180° first-order phase correction. Consequently, resonances which were folded in the F_2 dimension of the HCCH-TOCSY spectrum had opposite phase to unfolded resonances (Bax et al., 1991). The HCCH-COSY spectrum was acquired so that no phase correction was necessary in the F_2 dimension (Bax et al., 1990a; Clore et al., 1990).

Data processing in the F_1 and F_3 dimensions was performed using FTNMR (Hare Research); processing in the F_2 dimension was performed using a separate FORTRAN routine. Weak Lorentz-to-Gaussion transformation and cosine bell apodization was employed in all three dimensions; typically the data were zero filled once or twice in each dimension prior to Fourier transformation.

Results

Analysis of the HCA(CO)N Spectrum. Sequence-specific assignments of the backbone ^1H and ^{15}N resonances of IIA^{glc} were obtained previously using principally 3D ^1H–^{15}N TOCSY-HMQC and NOESY-HMQC experiments (Fairbrother et al., 1991). Sequential assignments of the $^{13}C^{\alpha}$ resonances were then obtained by using a 3D HCA(CO)N triple-resonance experiment, which correlates the $^1H^{\alpha}$ and $^{13}C^{\alpha}$ chemical shifts of each residue with the amide ^{15}N chemical shift of the following residue in the polypeptide. This experiment not only gives assignments for the $^{13}C^{\alpha}$ resonances but also provides an important check on the accuracy of the previous sequential assignments. In the new constant-time version of the HCA(CO)N experiment (Palmer et al., 1992) used here, $^1H^{\alpha}$ magnetization is transferred initially to the directly bound $^{13}C^{\alpha}$ using an INEPT scheme. During the following constant-time period, which includes the $^{13}C^{\alpha}t_1$ evolution period, magnetization is transferred from the $^{13}C^{\alpha}$ to the directly bonded carbonyl ^{13}C and subsequently to the amide ^{15}N of the succeeding residue. Following evolution of the ^{15}N chemical shifts during the t_2 period, magnetization is transferred back to the originating $^1H^{\alpha}$, in a step-wise fashion via the ^{13}CO and $^{13}C^{\alpha}$ nuclei, for detection. The final 3D spectrum contains cross-peaks labeled with $^{13}C^{\alpha}$, ^{15}N, and $^1H^{\alpha}$ chemical shifts in F_1, F_2, and F_3 dimensions, respectively.

The advantage of using constant-time evolution for the HCA(CO)N experiment, compared to the original scheme (Ikura et al., 1990; Kay et al., 1990b), is that an absorptive line shape is obtained in the F_1 dimension (Powers et al., 1991). In the constant-time HCA(CO)N scheme employed here, spectra can be recorded with sufficiently high resolution in t_1 to obviate the need to extend the data by linear prediction.

Representative $F_1(^{13}C)$–$F_3(^1H)$ planes of the 3D HCA(CO)N spectrum at different $F_2(^{15}N)$ chemical shifts are shown in Figure 1. Of the expected 161 $^1H_i^{\alpha}$–$^{13}C_i^{\alpha}$–$^{15}N_{i+1}$ correlations, 147 were observed in the 3D spectrum. No correlations were observed for the 10 N-terminal residues; similarly, none of the spin systems previously identified (Fairbrother et al., 1991) for residues 1–10 could be found in the HCCH-COSY or HCCH-TOCSY spectra [an exception to this was the spin system identified in the earlier work as Gln 7, which is now reassigned to the previously unidentified Gln 32 on the basis of sequential connectivities observed from Asp 31 and to Val 33 in the HCA(CO)N spectrum (Figure 1)]. Both results suggest that, in contrast to the uniformly ^{15}N-labeled sample used previously (Fairbrother et al., 1991), the $^{15}N/^{13}C$ double-labeled protein used in the present work is missing the initial N-terminal residues of IIA^{glc}. Subsequent to these observations, N-terminal sequencing indicated that residues 1–8 were indeed proteolyzed during preparation of the sample for NMR spectroscopy. The $^1H^{\alpha}$ and amide ^{15}N chemical shifts (after accounting for the 0.7 ppm upfield ^{15}N isotope shift between H_2O and D_2O solutions) of all the other assigned residues were found to be within experimental uncertainty of the previously reported values (Fairbrother et al., 1991). ^{15}N relaxation experiments show that the first 13 residues are disordered in solution (Stone et al., 1992), and the absence of medium- or long-range NOE connectivities (Fairbrother et al., 1991) indicates that they do not interact with the remainder of the protein; thus deletion of the 10 N-terminal residues from the $^{15}N/^{13}C$ double-labeled sample does not significantly affect the structure of the protein.

Analysis of the HCA(CO)N spectrum also revealed three sequential cross-peaks that were inconsistent with previous amide chemical shift assignments made for residues Val 56 and Arg 57 on the basis of NOE connectivities observed in ^1H–^{15}N NOESY-HMQC spectra. These cross-peaks, with $F_1(^{13}C^{\alpha})$, $F_2(^{15}N)$, and $F_3(^1H^{\alpha})$ chemical shifts of (61.0, 103.6, 4.60), (56.2, 122.0, 4.84), and (53.0, 114.8, 4.77), together with unambiguous identification of the spin systems corresponding to the $F_1(^{13}C^{\alpha})$–$F_3(^1H^{\alpha})$ cross-peaks from the HCCH-COSY and HCCH-TOCSY spectra, indicated that

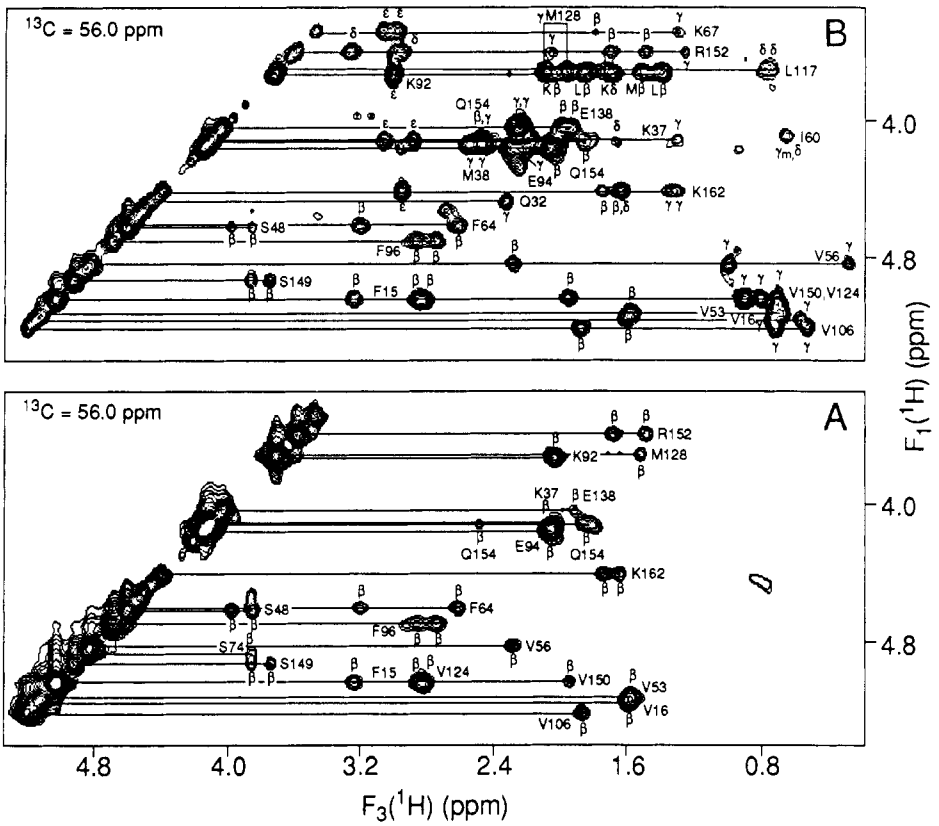

FIGURE 2: Expanded sections taken from the HCCH-COSY (A) and HCCH-TOCSY (B) spectra of uniformly $^{15}N/^{13}C$-labeled IIA^{glc} at $F_2(^{13}C^{\alpha})$ = 56.0 ppm, illustrating typical correlations originating from the $^1H^{\alpha}(F_1)$ of various amino acids. Specific assignments are indicated.

the previous amide ^1H and ^{15}N shifts of Val 56 and Arg 57 should be exchanged (see, for example, the cross-peaks assigned to Val 56 in Figures 1A, 2, and 3). In the previous work, no cross-peaks were observed at the amide frequencies of Val 56 and Arg 57 in the TOCSY-HMQC spectrum; consequently, the assignments for these residues were based solely upon cross-peaks in the NOESY-HMQC spectrum. The advantage of using scalar rather than dipolar correlations for sequential assignment purposes is emphasized by this example.

Analysis of HCCH-COSY and HCCH-TOCSY Spectra. Assignments of the aliphatic ^1H and ^{13}C resonances were completed using HCCH-COSY and HCCH-TOCSY experiments in conjunction with the HCA(CO)N experiment. Table I lists the ^1H, ^{15}N, and ^{13}C assignments for residues 11–162 of IIA^{glc}. In the HCCH experiments, ^1H magnetization that has been frequency labeled during the t_1 period is transferred from the ^1H nucleus to its directly bound ^{13}C nucleus via the $^1J_{CH}$ coupling (~140 Hz). Following evolution of the ^{13}C chemical shift during the t_2 period, magnetization is transferred through the ^{13}C spin system via the $^1J_{CC}$ couplings (~40 Hz) by using a 90° ^{13}C COSY mixing pulse in the HCCH-COSY experiment or isotropic mixing of the ^{13}C spins in the HCCH-TOCSY experiment. Finally, ^{13}C magnetization is transferred back to the directly attached ^1H via the $^1J_{CH}$ coupling. The resulting 3D spectrum has the appearance of a 2D ^1H–^1H COSY or TOCSY spectrum $[F_1(^1H)$–$F_3(^1H)]$ that has been edited in F_2 according to the ^{13}C chemical shift of the ^{13}C nucleus directly bound to the ^1H from which magnetization originates.

Starting with the assignments of the $^{13}C^{\alpha}$ and/or $^1H^{\alpha}$ resonances, most of the side-chain proton resonances can be identified in the $F_1(^1H^{\alpha})$–$F_2(^{13}C^{\alpha})$–$F_3(^1H)$ region of the HCCH-COSY and HCCH-TOCSY spectra. Figure 2 shows correlations that are observed in $F_1(^1H^{\alpha})$–$F_3(^1H)$ slices through the spectra at a $F_2(^{13}C^{\alpha})$ chemical shift of 56.0 ppm. The $^1H^{\beta}$ resonances can be distinguished from other ^1H resonances by comparison of the HCCH-COSY (Figure 2A) and HCCH-TOCSY (Figure 2B) spectra. The $^{13}C^{\beta}$ chemical shifts are found by locating the F_2 planes containing the symmetry related cross-peaks in the HCCH-COSY spectrum. This is illustrated for several Lys, Val, and Ile residues and for the AMX spin system of Phe 64 in Figure 3A. Since the frequency range of the aliphatic ^{13}C chemical shifts for different amino acid residues is limited (Clore et al., 1990; Ikura et al., 1991a), the process of searching for the appropriate $F_2(^{13}C)$ plane in the 3D spectra is greatly simplified. For AMX spin systems (F15, S48, F64, F96, and S149 in Figure 2), the only correlations observed are from the $^1H^{\alpha}$ to the corresponding $^1H^{\beta}$s. Serine spin systems can be easily distinguished from other AMX spin systems due to their characteristic $^{13}C^{\beta}$ chemical shifts (61–65 ppm); the $^1H^{\alpha}$ and $^1H^{\beta}$ shifts for Ser residues can be distinguished, even when the $^1H^{\beta}$ shifts are degenerate, because the $^{13}C^{\beta}$ shift is generally 2–10 ppm downfield from the $^{13}C^{\alpha}$ shift. Figure 4 shows correlations from the Ser $F_1(^1H^{\beta})$–$F_2(^{13}C^{\beta})$ region of the HCCH-COSY spectrum, in which the Ser $^1H^{\alpha}$ shift is either downfield from the $^1H^{\beta}$ shifts (S48, S126, S143, and S149) or between the $^1H^{\beta}$ shifts (S54), as well as an example where the $^1H^{\beta}$ shifts are degenerate (S143); obtaining assignments for these Ser spin systems would be difficult without knowledge of the $^{13}C^{\alpha}$ and $^{13}C^{\beta}$ chemical shifts.

Other spin systems which can generally be completely assigned using the HCCH-COSY spectrum include Ala, Gly, and Thr. The Gly $^1H^{\alpha}$s are attached to the same $^{13}C^{\alpha}$ and therefore give $F_1(^1H)$–$F_3(^1H)$ cross-peaks which are symmetrical about the diagonal, similar to those observed for β-methylene protons. In addition, the Gly $^{13}C^{\alpha}$ shifts are typically the most upfield of the $^{13}C^{\alpha}$s (41–46 ppm). Any β-methylene moieties that have $^{13}C^{\beta}$ chemical shifts similar to the $^{13}C^{\alpha}$ chemical shifts of Gly can be distinguished easily on

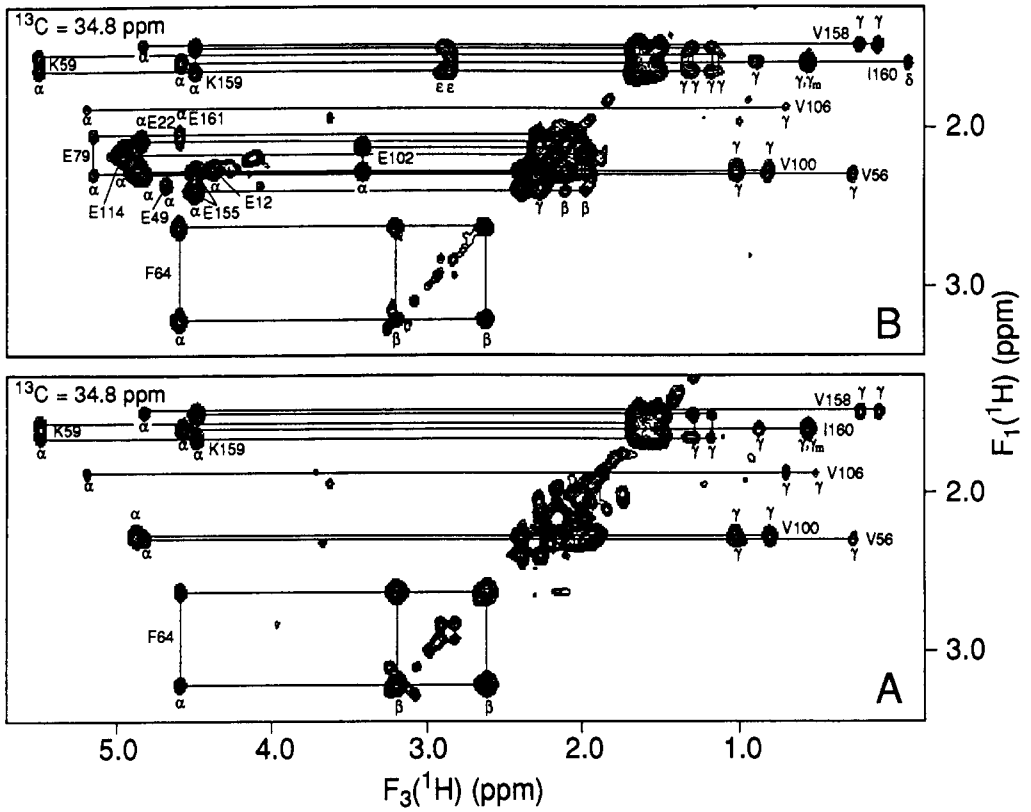

FIGURE 3: Expanded sections taken from the HCCH-COSY (A) and HCCH-TOCSY (B) spectra of uniformly $^{15}N/^{13}C$-labeled IIA^{glc} at $F_2(^{13}C^\beta)$ = 34.8 ppm, illustrating typical correlations originating from the $^1H^\beta(F_1)$ of various amino acids. Specific assignments are indicated.

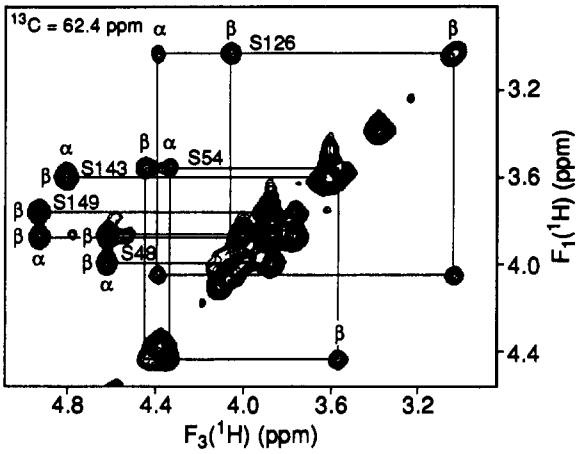

FIGURE 4: Expanded section of the HCCH-COSY spectrum of uniformly $^{15}N/^{13}C$-labeled IIA^{glc} at $F_2(^{13}C^\beta)$ = 62.4 ppm, illustrating correlations originating from Ser β-methylene protons (F_1). Specific assignments are indicated.

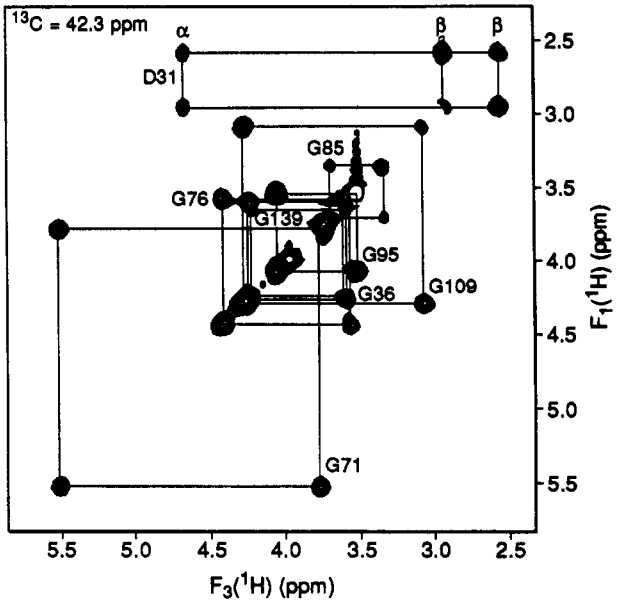

FIGURE 5: Expanded section of the HCCH-COSY spectrum of uniformly $^{15}N/^{13}C$-labeled IIA^{glc} at $F_2(^{13}C^\alpha)$ = 42.3 ppm, illustrating correlations observed for Gly residues. Also shown are the cross-peaks originating from the β-methylene protons of Asp 31; the $^{13}C^\beta$ resonance of Asp 31 is overlapped with the Gly $^{13}C^\alpha$ resonances.

the basis of the $F_1(^1H^\beta)$–$F_3(^1H^\alpha)$ cross-peaks of the former spin system. An example is shown in Figure 5, in which several Gly $^{13}C^\alpha$s share the same chemical shift as the $^{13}C^\beta$ resonance of Asp 31. The unique Ala and Thr spin systems can also be distuinguished on the basis of their ^{13}C chemical shifts. Alanine gives a single $F_1(^1H^\alpha)$–$F_3(^1H^\beta)$ cross-peak at a $F_2(^{13}C^\alpha)$ shift of ~50 ppm (see, for example, Figure 6A) with the symmetry related $F_1(^1H^\beta)$–$F_3(^1H^\alpha)$ cross-peak appearing at a $F_2(^{13}C^\beta)$ shift of ~19 ppm. The Thr spin systems are most readily identified by the correlations found in the $F_1(^1H^\beta)$–$F_2(^{13}C^\beta)$ region of the spectrum (Figure 6B), since the $F_2(^{13}C^\beta)$ shifts for Thr are typically the most downfield aliphatic shifts observed (65–72 ppm).

For side chains longer than AMX spin systems, the $^1H^\gamma$ shifts can be determined from the $F_1(^1H^\beta)$–$F_2(^{13}C^\beta)$ region of the HCCH-COSY (see, for example, Figure 3A). In the case of Glu, Gln, and Met residues, the difference between $^1H^\beta$ and $^1H^\gamma$ shifts and between $^{13}C^\beta$ and $^{13}C^\gamma$ shifts may be quite small. If the $^1H^\beta$ and $^1H^\gamma$ shifts cannot be distinguished in the $F_1(^1H^\alpha)$–$F_2(^{13}C^\alpha)$ regions of the HCCH spectra (due to cross-peak overlap, for instance), they can be identified on the basis of $F_1(^1H^\beta)$–$F_3(^1H^\alpha)$ cross-peaks observable at the $F_2(^{13}C^\beta)$ frequency in both the HCCH-COSY and HCCH-TOCSY spectra, and $F_1(^1H^\gamma)$–$F_3(^1H^\alpha)$ cross-peaks which are observable at the $F_2(^{13}C^\gamma)$ frequency only in the HCCH-TOCSY spectrum. Examples of the latter can be seen for Glu residues

Table I: ^{1}H, ^{15}N, and ^{13}C Chemical Shifts for IIA^{glc} at pH 6.6 and 308 K, with 10 mM Potassium Phosphate[a]

	NH	C^{α}	C^{β}	C^{γ}	C^{δ}/NH_2^{δ}	$C^{\epsilon}/NH_2^{\delta}$
Gly 11						
^{1}H	8.25	4.04, 3.94				
$^{15}N/^{13}C$	111.5	43.0				
Glu 12						
^{1}H	8.09	4.39	2.07, 1.96	2.28, 2.28		
$^{15}N/^{13}C$	120.8	54.6	28.2	33.9		
Glu 13						
^{1}H	8.49	4.51	2.09, 2.09	2.30, 2.30		
$^{15}N/^{13}C$	123.2	53.8	28.5	33.4		
Val 14						
^{1}H	8.31	4.12	2.05	1.03, 0.94		
$^{15}N/^{13}C$	125.3	61.0	30.2			
Phe 15						
^{1}H	8.10	5.03	3.26, 2.87			
$^{15}N/^{13}C$	127.3	55.6	38.8			
Val 16						
^{1}H	9.09	5.16	1.61	0.75, 0.57		
$^{15}N/^{13}C$	123.2	55.6	31.4	18.7, 15.9		
Ser 17						
^{1}H	8.61	4.37	4.58, 3.77			
$^{15}N/^{13}C$	110.2	54.6	62.9			
Pro 18						
^{1}H		4.66	2.35, 2.27	1.92, 1.89	4.22, 4.06	
$^{15}N/^{13}C$	142.1	61.4	32.5	24.5	48.0	
Ile 19						
^{1}H	7.17	4.62	1.37	1.59, 1.39, (1.14)[b]	0.92	
$^{15}N/^{13}C$	115.3	57.9	43.7	26.8 (15.6)	13.0	
Thr 20						
^{1}H	9.32	4.97	4.10	1.44		
$^{15}N/^{13}C$	125.0	59.0	69.2	19.3		
Gly 21						
^{1}H	8.80	4.72, 4.09				
$^{15}N/^{13}C$	115.3	43.7				
Glu 22						
^{1}H	8.07	4.85	2.18, 2.10	2.29, 2.10		
$^{15}N/^{13}C$	120.4	53.2	30.8	34.5		
Ile 23						
^{1}H	8.80	4.95	1.66	1.86, 1.27, (0.86)	0.70	
$^{15}N/^{13}C$	128.7	59.7	38.2	27.9 (12.4)	13.0	
His 24						
^{1}H	9.48	5.01	3.44, 2.66		7.12	8.53
$^{15}N/^{13}C$	125.1	51.6	30.8			
Pro 25						
^{1}H		5.02	2.50, 2.12	2.11, 1.96	4.04, 3.78	
$^{15}N/^{13}C$	131.7	60.1	30.2	25.0	48.3	
Ile 26						
^{1}H	9.48	3.82	1.59	1.40, 1.34, (1.16)	0.83	
$^{15}N/^{13}C$	122.8	60.7	37.1	27.9, (15.6)	12.4	
Thr 27						
^{1}H	7.09	4.15	4.52	1.43		
$^{15}N/^{13}C$	107.4	60.8	66.4	19.9		
Asp 28						
^{1}H	7.53	4.74	2.81, 2.74			
$^{15}N/^{13}C$	119.5	52.3	38.8			
Val 29						
^{1}H	7.41	3.80	2.09	0.82, 0.74		
$^{15}N/^{13}C$	121.7	59.5	29.6	19.9, 22.2		
Pro 30						
^{1}H		4.82	2.38, 1.85	2.11, 1.83	3.84, 3.29	
$^{15}N/^{13}C$	142.0	60.4	25.6	25.3	48.6	
Asp 31						
^{1}H	8.29	4.69	2.96, 2.58			
$^{15}N/^{13}C$	123.5	51.8	42.3			
Gln 32						
^{1}H	8.34	4.49	2.09, 1.98	2.29, 2.29		7.43, 6.74
$^{15}N/^{13}C$	121.3	55.3				111.5
Val 33						
^{1}H	7.90	3.73	1.65	0.79, 0.33		
$^{15}N/^{13}C$	120.0	63.6	29.6	19.3, 18.2		
Phe 34						
^{1}H	9.18	4.36	2.90, 2.65			
$^{15}N/^{13}C$	119.2	59.1	36.8			
Ser 35						
^{1}H	9.32	4.26	4.49, 3.97			
$^{15}N/^{13}C$	116.4	58.7	61.2			
Gly 36						
^{1}H	7.36	4.26, 3.60				
$^{15}N/^{13}C$	107.0	42.6				
Lys 37						
^{1}H	8.07	4.12	2.08	1.31	1.70, 1.67	3.07, 2.90
$^{15}N/^{13}C$	112.9	56.0		23.9	27.9	40.3

Table I (Continued)

	NH	C^α	C^β	C^γ	C^δ/NH_2^δ	C^ϵ/NH_2^δ
Met 38						
^1H	7.84	4.15	2.12, 2.06	2.57, 2.47		
$^{15}N/^{13}C$	116.4	56.5	29.9	30.5		
Met 39						
^1H	8.24	4.57	2.06, 1.94	2.28		
$^{15}N/^{13}C$	114.7	52.3	30.2			
Gly 40						
^1H	6.74	4.65, 3.74				
$^{15}N/^{13}C$	105.1	41.7				
Asp 41						
^1H	7.37	5.00	2.88, 2.72			
$^{15}N/^{13}C$	117.6	50.2	40.5			
Gly 42						
^1H	9.22	5.28, 4.05				
$^{15}N/^{13}C$	106.3	45.3				
Phe 43						
^1H	9.16	4.89	3.29, 3.15			
$^{15}N/^{13}C$	119.6	53.5	37.1			
Ala 44						
^1H	9.26	5.20	0.81			
$^{15}N/^{13}C$	120.8	48.2	21.0			
Ile 45						
^1H	8.05	5.03	1.21	1.66, (0.40)	0.94	
$^{15}N/^{13}C$	118.1	56.7	40.5	(14.1)	12.1	
Leu 46						
^1H	9.44	4.85	2.22, 1.29	1.45	0.90, 0.81	
$^{15}N/^{13}C$	131.6	49.4	40.3	25.6	22.8, 21.3	
Pro 47						
^1H		4.61	2.46, 1.96	1.95, 1.59	4.43, 3.28	
$^{15}N/^{13}C$	142.0	61.4	31.4	25.6	50.9	
Ser 48						
^1H	9.54	4.60	4.00, 3.88			
$^{15}N/^{13}C$	115.5	55.7	62.4			
Glu 49						
^1H	7.42	4.70	2.25, 1.95	2.36, 2.36		
$^{15}N/^{13}C$	118.1	52.8	31.9	34.5		
Gly 50						
^1H	9.57	4.23, 4.17				
$^{15}N/^{13}C$	112.2	43.8				
Ile 51						
^1H	6.81	4.61	1.61	1.60, 1.10, (0.78)	0.83	
$^{15}N/^{13}C$	118.9	58.8	38.2	25.6, (15.3)	10.4	
Val 52						
^1H	8.85	4.96	2.08	1.01, 0.98		
$^{15}N/^{13}C$	127.2	58.4	31.4	18.4, 19.3		
Val 53						
^1H	9.78	5.12	1.58	0.73, 0.69		
$^{15}N/^{13}C$	122.4	55.6	31.9	15.9, 18.7		
Ser 54						
^1H	8.73	4.33	4.43, 3.55			
$^{15}N/^{13}C$	110.4	53.7	62.4			
Pro 55						
^1H		4.60	1.83, 1.83	1.75, 1.60	3.87, 3.87	
$^{15}N/^{13}C$	135.5	61.0	31.4	23.9	47.7	
Val 56						
^1H	7.00	4.84	2.30	1.02, 0.30		
$^{15}N/^{13}C$	103.6	56.2	34.5	20.2, 14.7		
Arg 57						
^1H	8.76	4.77	1.95, 1.95	1.76, 1.76	3.34, 3.26	
$^{15}N/^{13}C$	122.0	53.0	28.8	26.2	41.4	
Gly 58						
^1H	8.33	4.45, 4.27				
$^{15}N/^{13}C$	114.8	44.6				
Lys 59						
^1H	8.85	5.52	1.66, 1.58	1.36, 1.12	1.60, 1.60	2.86, 2.86
$^{15}N/^{13}C$	121.2	51.7	34.2	21.6	27.1	39.4
Ile 60						
^1H	8.79	4.08	2.39	1.82, 1.13, (0.68)	0.65	
$^{15}N/^{13}C$	121.0	56.6	32.8	23.3, (15.6)	7.5	
Leu 61						
^1H	9.04	4.42	1.43, 1.43	1.43	0.81, 0.77	
$^{15}N/^{13}C$	130.0	53.7	41.4		23.0, 19.3	
Asn 62						
^1H	7.70	4.85	2.44, 2.43		7.13, 6.11	
$^{15}N/^{13}C$	113.2	51.1	39.4		110.4	
Val 63						
^1H	8.78	4.34	2.06	0.96, 0.79		
$^{15}N/^{13}C$	124.2	60.0	30.5	17.6, 18.2		
Phe 64						
^1H	8.20	4.60	3.22, 2.62			
$^{15}N/^{13}C$	126.6	55.6	34.8			

Table I (Continued)

	NH	C^{α}	C^{β}	C^{γ}	C^{δ}/NH_2^{δ}	$C^{\epsilon}/NH_2^{\delta}$
Pro 65						
^1H		4.42	2.49, 2.07	2.20, 2.16	3.94, 3.94	
$^{15}N/^{13}C$	136.8	63.8	29.6	25.3	48.6	
Thr 66						
^1H	7.18	4.07	4.83	1.22		
$^{15}N/^{13}C$	102.5	60.1	65.2	19.3		
Lys 67						
^1H	8.37	3.49	2.04, 1.81	1.31, 1.31	1.82, 1.49	3.08, 3.00
$^{15}N/^{13}C$	113.3	56.4	27.9	22.8	27.1	40.0
His 68						
^1H	6.95	3.96	2.87, 1.20		5.42	7.27
$^{15}N/^{13}C$	109.5	54.0	28.8			
Ala 69						
^1H	6.22	5.02	−0.02			
$^{15}N/^{13}C$	117.6	47.0	18.2			
Ile 70						
^1H	8.41	4.77	1.51	1.54, 1.08, (0.89)	0.79	
$^{15}N/^{13}C$	118.9	57.1	41.4	25.6, (15.0)	12.4	
Gly 71						
^1H	9.31	5.52, 3.79				
$^{15}N/^{13}C$	113.2	42.1				
Leu 72						
^1H	9.73	5.16	1.47, 1.46	1.55	0.69, 0.67	
$^{15}N/^{13}C$	124.7	52.9	44.6	25.0	25.3, 25.3	
Gln 73						
^1H	8.96	5.43	1.98, 1.86	2.44, 2.07		7.69, 6.73
$^{15}N/^{13}C$	120.4	51.6	31.1	31.7		111.3
Ser 74						
^1H	10.07	4.85	4.78, 3.86			
$^{15}N/^{13}C$	126.1	56.0	62.9			
Asp 75						
^1H	8.39	4.57	2.15, 1.85			
$^{15}N/^{13}C$	121.1					
Gly 76						
^1H	8.14	4.44, 3.58				
$^{15}N/^{13}C$	108.2	42.3				
Gly 77						
^1H	8.93	4.15, 3.68				
$^{15}N/^{13}C$	107.3	42.8				
Arg 78						
^1H	8.23	4.61	2.15, 1.85	1.79, 1.79	3.15, 3.03	
$^{15}N/^{13}C$	122.1	53.7	27.9	24.5	40.8	
Glu 79						
^1H	8.93	5.15	1.87, 1.71	2.30, 2.07		
$^{15}N/^{13}C$	125.2	53.9	27.9	35.7		
Ile 80						
^1H	8.90	5.07	1.33	1.40, 0.65, (0.49)	0.82	
$^{15}N/^{13}C$	124.4	57.2	41.4	25.6 (15.0)	13.6	
Leu 81						
^1H	9.56	5.20	1.72, 1.51	1.27	0.94, 0.83	
$^{15}N/^{13}C$	130.3	51.5	43.1	25.6	23.3, 20.5	
Ile 82						
^1H	8.72	4.45	1.65	1.56, 0.85, (0.67)	0.62	
$^{15}N/^{13}C$	125.0	58.7	37.7	24.8, (13.3)	11.3	
His 83						
^1H	8.04	4.61	2.75, 2.32		6.71	7.87
$^{15}N/^{13}C$	128.5	52.5	27.9			
Phe 84						
^1H	9.14	4.49	3.60, 2.44			
$^{15}N/^{13}C$	127.1	57.0	38.0			
Gly 85						
^1H	7.60	3.71, 3.35				
$^{15}N/^{13}C$	118.9	42.8				
Ile 86						
^1H	7.18	4.66	1.89	1.83, 0.92, (0.99)	0.63	
$^{15}N/^{13}C$	113.3	54.6	36.2	(15.3)	7.3	
Asp 87						
^1H	9.05	4.53	3.17, 2.71			
$^{15}N/^{13}C$	120.0	54.0	37.4			
Thr 88						
^1H	7.94	3.79	4.04	1.55		
$^{15}N/^{13}C$	107.8	60.5	65.2	23.3		
Val 89						
^1H	8.32	3.38	1.80	0.99, 0.81		
$^{15}N/^{13}C$	124.5	62.2	28.5	19.0, 17.3		
Ser 90						
^1H	7.36	4.16	4.01, 3.98			
$^{15}N/^{13}C$	116.4	58.3	61.8			
Leu 91						
^1H	7.31	4.35	2.22, 2.07	1.81	1.19, 0.98	
$^{15}N/^{13}C$	120.3	53.2	38.2	25.9	24.2, 21.3	

Table I (Continued)

	NH	C^α	C^β	C^γ	$C^\delta/NH_2{}^\delta$	$C^\epsilon/NH_2{}^\delta$
Lys 92						
^1H	8.12	3.74	2.06, 2.06	1.39, 1.39	1.71, 1.71	3.01, 3.01
$^{15}N/^{13}C$	114.9	55.7	27.3	22.5	26.8	39.7
Gly 93						
^1H	9.13	4.25, 3.86				
$^{15}N/^{13}C$	107.0	43.1				
Glu 94						
^1H	7.71	4.16	2.10, 2.08	2.32, 2.27		
$^{15}N/^{13}C$	123.6	55.8	26.5	33.7		
Gly 95						
^1H	8.45	4.07, 3.54				
$^{15}N/^{13}C$	110.9	42.3				
Phe 96						
^1H	7.72	4.70	2.87, 2.76			
$^{15}N/^{13}C$	118.3	55.9	40.5			
Thr 97						
^1H	8.74	4.41	3.91	0.77		
$^{15}N/^{13}C$	118.2	59.8	69.2	19.0		
Ser 98						
^1H	8.71	5.15	3.77, 3.76			
$^{15}N/^{13}C$	119.3	54.4	63.5			
Phe 99						
^1H	8.30	4.56	3.47, 2.42			
$^{15}N/^{13}C$	120.8	56.5	38.2			
Val 100						
^1H	7.61	4.90	2.28	1.05, 0.83		
$^{15}N/^{13}C$	110.1	56.9	34.8	20.2, 15.3		
Ser 101						
^1H	8.76	4.66	3.81, 3.59			
$^{15}N/^{13}C$	115.9	54.6	64.1			
Glu 102						
^1H	8.79	3.43	1.97, 1.86	2.28, 2.13		
$^{15}N/^{13}C$	121.9	57.1	26.5	34.2		
Gly 103						
^1H	8.66	4.45, 3.57				
$^{15}N/^{13}C$	113.7	42.9				
Asp 104						
^1H	7.87	4.51	2.73, 2.55			
$^{15}N/^{13}C$	121.1	53.4	38.8			
Arg 105						
^1H	8.50	4.88	2.02, 1.83	1.85, 1.79	3.23, 3.23	
$^{15}N/^{13}C$	121.0	52.8	27.9	24.5	40.0	
Val 106						
^1H	8.68	5.21	1.89	0.72, 0.53		
$^{15}N/^{13}C$	113.6	56.3	33.7	19.9, 15.3		
Glu 107						
^1H	7.42	4.78	2.12, 1.59	2.35, 2.24		
$^{15}N/^{13}C$	120.7	50.7	28.5	33.1		
Pro 108						
^1H		3.85	1.81, 1.76	2.12, 1.66	3.73, 3.36	
$^{15}N/^{13}C$	134.9	60.8	27.9	25.6	48.0	
Gly 109						
^1H	9.48	4.30, 3.09				
$^{15}N/^{13}C$	111.1	42.6				
Gln 110						
^1H	7.93	4.09	2.26, 1.80	2.43, 2.43		7.59, 6.97
$^{15}N/^{13}C$	122.2	54.1	27.3	33.4		109.9
Lys 111						
^1H	8.75	3.82	1.45, 1.45	1.16, 0.80	1.11, 1.11	2.27, 1.57
$^{15}N/^{13}C$	127.6	57.7	29.6	22.8	26.8	38.2
Leu 112						
^1H	9.30	4.68	1.58, 1.35	1.84	0.78, 0.70	
$^{15}N/^{13}C$	121.5	53.6	42.3	24.5	22.2, 23.9	
Leu 113						
^1H	7.79	5.56	1.48, 1.38	1.40	0.88, 0.86	
$^{15}N/^{13}C$	116.9	51.7	46.9	24.8	21.6, 21.6	
Glu 114						
^1H	9.02	4.97	1.99, 1.99	2.17, 2.17		
$^{15}N/^{13}C$	121.3	53.6	31.7	35.1		
Val 115						
^1H	8.69	4.27	1.07	−0.18, −0.27		
$^{15}N/^{13}C$	124.9	57.9	31.9	18.2, 17.0		
Asp 116						
^1H	8.45	4.58	2.82, 2.42			
$^{15}N/^{13}C$	126.1	50.0	37.4			
Leu 117						
^1H	8.23	3.70	1.89, 1.42	1.75	0.80, 0.75	
$^{15}N/^{13}C$	125.2	56.6	39.1		20.7, 22.8	

Table I (Continued)

	NH	C^{α}	C^{β}	C^{γ}	C^{δ}/NH_2^{δ}	$C^{\epsilon}/NH_2^{\delta}$
Asp 118						
^1H	8.03	4.35	2.70, 2.58			
$^{15}N/^{13}C$	116.4	55.0	38.2			
Ala 119						
^1H	7.21	4.19	1.34			
$^{15}N/^{13}C$	119.7	51.0	16.4			
Val 120						
^1H	7.61	3.88	1.74	0.87, 0.73		
$^{15}N/^{13}C$	116.0	63.6	31.9	19.3, 19.9		
Lys 121						
^1H	8.43	3.95	2.01, 1.97	1.47, 1.39	1.68, 1.68	2.95, 2.95
$^{15}N/^{13}C$	118.6	59.8	28.5	23.0	27.3	39.7
Pro 122						
^1H		4.52	2.35, 1.68	1.93, 1.93	3.69, 3.22	
$^{15}N/^{13}C$	132.7	63.1	29.1	25.3	48.6	
Asn 123						
^1H	7.85	4.91	3.08, 2.58		7.09, 7.08	
$^{15}N/^{13}C$	112.0	51.6	40.0		114.9	
Val 124						
^1H	7.25	5.05	2.84	0.90, 0.72		
$^{15}N/^{13}C$	110.6	56.0	30.8	21.0, 15.6		
Pro 125						
^1H		4.37	2.40, 1.83	2.19, 1.96	4.16, 3.87	
$^{15}N/^{13}C$	133.5	62.3	30.2	25.0	48.6	
Ser 126						
^1H	6.67	4.39	4.06, 3.04			
$^{15}N/^{13}C$	105.6	54.9	62.6			
Leu 127						
^1H	8.68	4.26	1.58, 1.52	1.75	0.96, 0.83	
$^{15}N/^{13}C$	123.8	51.8	40.5	23.9	24.2, 21.0	
Met 128						
^1H	8.52	3.72	1.54, 1.54	2.11, 1.97		1.32
$^{15}N/^{13}C$	120.8	55.8	29.6	31.4		14.1
Thr 129						
^1H	7.95	4.98	4.14	0.88		
$^{15}N/^{13}C$	121.4	58.7	71.0	17.0		
Pro 130						
^1H		4.21	1.50, 1.15	0.60, 0.60	4.54, 3.46	
$^{15}N/^{13}C$	139.0	59.6	31.4	24.5	49.1	
Ile 131						
^1H	8.53	4.46	0.44	1.21, 0.76, (0.42)	0.51	
$^{15}N/^{13}C$	124.9	58.9	35.4	27.1, (17.0)	13.3	
Val 132						
^1H	8.80	4.59	1.89	0.86, 0.71		
$^{15}N/^{13}C$	120.3	57.9	33.1	18.7, 20.2		
Phe 133						
^1H	9.21	5.23	3.22, 2.98			
$^{15}N/^{13}C$	125.1	54.6	36.5			
Thr 134						
^1H	8.35	4.61	4.59	1.19		
$^{15}N/^{13}C$	113.4	61.2	66.9	19.3		
Asn 135						
^1H	8.22	5.18	3.11, 2.65		7.88, 7.33	
$^{15}N/^{13}C$	122.1	49.9	36.2		112.2	
Leu 136						
^1H	8.46	4.18	1.87, 1.70	1.83	0.85, 0.72	
$^{15}N/^{13}C$	120.3	53.9	38.8	24.2	23.9, 20.5	
Ala 137						
^1H	8.97	4.38	1.34			
$^{15}N/^{13}C$	125.1	48.7	17.0			
Glu 138						
^1H	8.52	4.04	2.02, 1.95	2.27, 2.27		
$^{15}N/^{13}C$	121.4	56.4	26.8	33.7		
Gly 139						
^1H	8.73	4.25, 3.68				
$^{15}N/^{13}C$	113.5	42.8				
Glu 140						
^1H	7.81	4.83	2.35, 1.65	2.18, 1.97		
$^{15}N/^{13}C$	119.6	54.3	29.1	36.5		
Thr 141						
^1H	8.76	4.66	4.08	1.12		
$^{15}N/^{13}C$	114.1	57.9	70.4	18.7		
Val 142						
^1H	8.30	4.13	1.97	0.66, 0.66		
$^{15}N/^{13}C$	121.9	60.0	30.2	19.3, 18.7		
Ser 143						
^1H	8.90	4.80	3.61, 3.61			
$^{15}N/^{13}C$	123.3	54.1	62.6			
Ile 144						
^1H	8.76	4.05	1.82	1.67, 0.88, (0.93)	0.98	

Table I (Continued)

	NH	C^α	C^β	C^γ	C^δ/NH_2^δ	C^ϵ/NH_2^δ
$^{15}N/^{13}C$	125.3	60.3	36.0	25.0, (15.9)	11.3	
Lys 145						
^1H	8.34	4.35	1.79, 1.50	1.22, 1.14	1.41, 1.41	2.79, 2.68
$^{15}N/^{13}C$	125.8	53.1	30.2	21.6	25.6	39.7
Ala 146						
^1H	7.15	4.54	1.33			
$^{15}N/^{13}C$	121.4	49.0	18.7			
Ser 147						
^1H	8.04	4.43	3.70, 3.70			
$^{15}N/^{13}C$	111.2	54.8	63.5			
Gly 148						
^1H	8.71	4.10, 3.71				
$^{15}N/^{13}C$	111.1	43.4				
Ser 149						
^1H	8.33	4.92	3.88, 3.76			
$^{15}N/^{13}C$	120.3	56.4	62.1			
Val 150						
^1H	9.31	5.04	1.96	0.91, 0.81		
$^{15}N/^{13}C$	118.1	56.3	33.1	16.4, 20.5		
Asn 151						
^1H	8.16	5.39	2.68, 2.57		7.57, 6.87	
$^{15}N/^{13}C$	119.1	49.3	40.0		113.8	
Arg 152						
^1H	8.63	3.60	1.71, 1.52	2.08, 1.28	3.27, 2.97	
$^{15}N/^{13}C$	120.7	55.9	28.2	25.0	41.7	
Glu 153						
^1H	9.49	3.23	2.46, 2.26	1.96, 1.87		
$^{15}N/^{13}C$	113.5	57.4	25.6	37.1		
Gln 154						
^1H	8.01	4.12	2.51, 1.82	2.50, 2.50		7.91, 7.24
$^{15}N/^{13}C$	121.7	55.7	27.3	30.8		111.3
Glu 155						
^1H	8.82	4.51	2.11, 1.99	2.40, 2.28		
$^{15}N/^{13}C$	125.6	54.3	29.1	34.5		
Asp 156						
^1H	8.87	4.49	2.96, 2.56			
$^{15}N/^{13}C$	117.1	53.5	37.1			
Ile 157						
^1H	7.84	4.16	1.67	1.48, 1.22, (0.84)	0.92	
$^{15}N/^{13}C$	108.2	61.0	36.5	23.9, (16.7)	12.1	
Val 158						
^1H	7.64	4.84	1.51	0.26, 0.13		
$^{15}N/^{13}C$	114.3	57.0	33.7	16.4, 18.2		
Lys 159						
^1H	8.67	4.50	1.68, 1.52	1.31, 1.19	1.66, 1.66	2.94, 2.88
$^{15}N/^{13}C$	121.8	52.6	34.5	22.5	26.5	39.7
Ile 160						
^1H	8.57	4.59	1.62	0.89, 0.57, (0.58)	−0.07	
$^{15}N/^{13}C$	124.7	57.8	34.5	25.0, (15.9)	9.0	
Glu 161						
^1H	8.88	4.62	2.00, 1.76	2.11, 2.04		
$^{15}N/^{13}C$	128.7	53.1	30.2	33.9		
Lys 162						
^1H	7.83	4.41	1.77, 1.67	1.38, 1.32	1.66, 1.66	2.97, 2.97
$^{13}N/^{13}C$	124.7	55.5	32.5	22.5	27.1	40.0

[a] ^1H and ^{13}C chemical shifts are relative to TMS; ^{15}N chemical shifts are relative to liquid NH_3. [b] Values in parentheses correspond to Ile $C^\gamma H_3$.

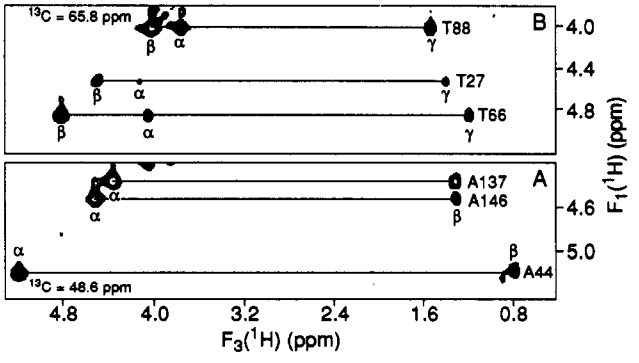

FIGURE 6: Expanded sections of the HCCH-COSY spectrum of uniformly $^{15}N/^{13}C$-labeled IIA^{glc} illustrating correlations observed from the $^1H^\alpha$ (F_1) of Ala residues at $F_2(^{13}C^\alpha)$ = 48.6 ppm (A) and from the $^1H^\beta(F_1)$ of Thr residues at $F_2(^{13}C^\beta)$ = 65.8 ppm (B).

(E12, E22, E49, E79, E102, E114, E155, and E161) in Figure 3B.

Among the more difficult amino acid side chains to assign by conventional 2D homonuclear NMR methods are Arg, Lys, and Pro, because coherence transfer via weak ^1H–^1H ^3J couplings is ineffective, and because overlap is common for $^1H^\beta$ and $^1H^\gamma$ shifts in the case of Arg and Pro, and $^1H^\beta$, $^1H^\gamma$, and $^1H^\delta$ shifts in the case of Lys. Figure 7 shows regions of the HCCH-COSY and HCCH-TOCSY spectra used for assignment of Lys 111. Comparison of the HCCH-COSY and HCCH-TOCSY spectra at the $F_2(^{13}C^\alpha)$ frequency (Figure 7, panels A and B, respectively) reveals that the $^1H^\beta$ chemical shifts of this spin system are degenerate at 1.45 ppm. Assignment of the $^{13}C^\beta$ frequency leads to identification of the $^1H^\gamma$ shifts, by comparison of the HCCH-COSY and HCCH-TOCSY spectra (Figure 7, panels C and D, respectively). The HCCH-TOCSY spectrum at the $F_2(^{13}C^\delta)$ shift (Figure 7E) shows that the $^1H^\delta$ shifts are degenerate and overlapped with the downfield $^1H^\gamma$ resonance, while the slice at the F_2-($^{13}C^\epsilon$) shift (Figure 7E) confirms the rather unusual $^1H^\epsilon$

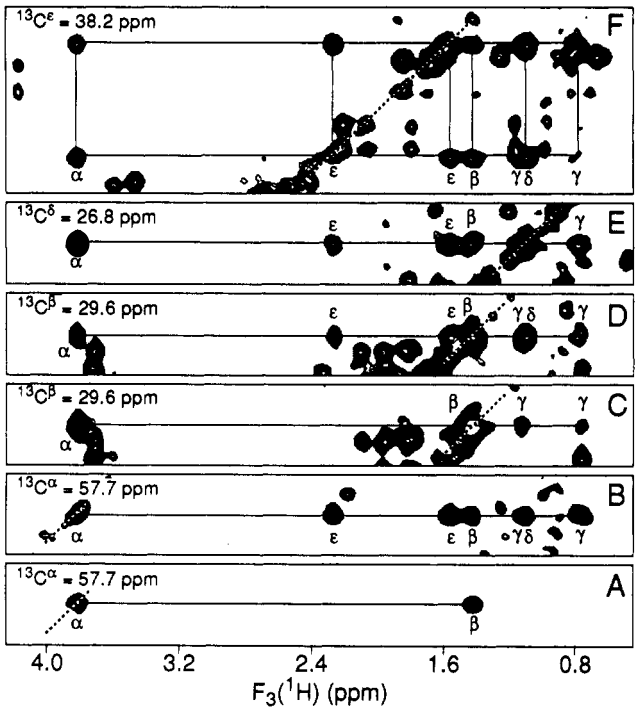

FIGURE 7: Selection of slices from the HCCH-COSY (A and C) and the HCCH-TOCSY (B, D, E, and F) spectra of uniformly $^{15}N/^{13}C$-labeled IIA^{glc}, illustrating the assignment of Lys 111. The dotted lines defines the diagonal and, therefore, the $F_1(^1H)$ shift of the labeled cross-peaks.

chemical shifts for Lys 111. The aliphatic chemical shifts found for Lys 111 suggest that it is in a unique environment (possibly involving hydrogen bonding) relative to the other Lys residues in the protein. Using the HCCH spectra, the side-chain resonances of the four Arg and nine Lys residues were completely assigned, with the exception of the $^{13}C^{\beta}$ shift of Lys 37. None of the Arg or Lys side chains were assigned previously beyond the β-methylene protons (Fairbrother et al., 1991).

Example regions of the HCCH-COSY and HCCH-TOCSY spectra used to assign the Pro residues are illustrated in Figure 8. In both cases shown, Pro 25 and Pro 30, a $^1H^{\beta}$ resonance overlaps with a $^1H^{\gamma}$ resonance. As above, the $^1H^{\beta}$ shifts can be distinguished from the $^1H^{\gamma}$ shifts by comparison of the HCCH-COSY and HCCH-TOCSY spectra at the $F_2(^{13}C^{\alpha})$ frequency (Figure 8, panels A and B, respectively). The Pro spin systems are easily distinguished from the identical Arg spin systems on the basis of their differing $^{13}C^{\alpha}$ and $^{13}C^{\delta}$ chemical shifts (~62 and 48 ppm, respectively, for Pro, and ~55 and 42 ppm, respectively, for Arg). Correlations observable in the Pro $F_2(^{13}C^{\delta})$ region of the HCCH-TOCSY spectra are shown in Figure 8C. Despite the cross-peak overlap observed in this region of the spectrum, the 10 Pro residues of IIA^{glc} were completely assigned (excluding Pro 5 in the missing N-terminal region).

Discussion

Virtually complete aliphatic ^1H and ^{13}C assignments have been determined for the IIA^{glc} domain of *B. subtilis* (Table I) by using 3D HCCH-COSY and HCCH-TOCSY experiments in conjunction with the 3D triple-resonance HCA(CO)N experiment. The HCA(CO)N experiment was used to correlate the $^{13}C^{\alpha}$ chemical shifts with the $^1H^{\alpha}$ and amide ^{15}N chemical shifts, assigned previously using principally 3D ^1H–^{15}N NOESY-HMQC and TOCSY-HMQC spectra (Fairbrother et al., 1991). The amino acid spin systems identified using the HCCH-COSY and HCCH-TOCSY

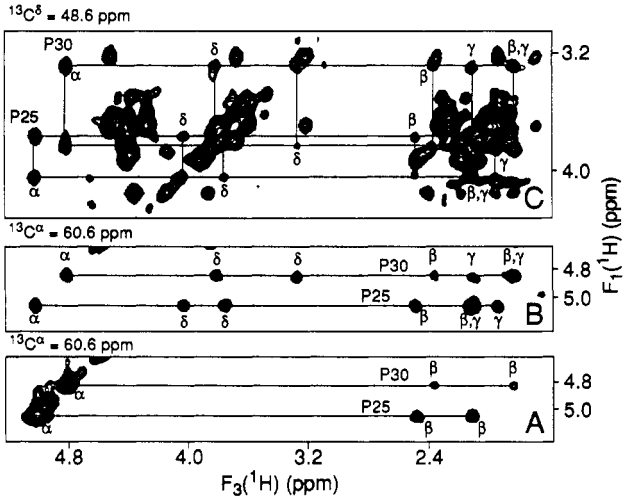

FIGURE 8: Selection of slices from the HCCH-COSY (A) and the HCCH-TOCSY (B and C) spectra of uniformly $^{15}N/^{13}C$-labeled IIA^{glc}, illustrating the assignment of Pro 25 and Pro 30.

spectra were then sequentially assigned on the basis of their $^1H^{\alpha}$ and $^{13}C^{\alpha}$ chemical shifts, together with the amino acid sequence. The strategy used here is similar to that employed by Clore and co-workers in the assignment of interleukin-1β (Driscoll et al., 1990; Clore et al., 1990), with the exception that, in the present work, the 3D triple-resonance HCA(CO)N rather than the HNCA experiment was used to assign the $^{13}C^{\alpha}$ chemical shifts. One advantage of using the HCA(CO)N experiment is that it can be acquired using the same D_2O solution used for the HCCH-COSY and HCCH-TOCSY experiments. In addition, it provides an unambiguous intraresidue correlation between the $^1H^{\alpha}$ and the $^{13}C^{\alpha}$ resonances, both of which facilitate the sequential assignment of spin systems identified in the HCCH-COSY and HCCH-TOCSY spectra. The HNCA experiment provides both intraresidue and usually weaker sequential interresidue correlations between $^{13}C^{\alpha}$ and amide ^1H and ^{15}N resonances and is an equally valid method for obtaining the $^{13}C^{\alpha}$ chemical shift assignments. Both experiments may be necessary to avoid any problems due to ambiguity of the $^1H^{\alpha}$ chemical shifts; however, in the case of IIA^{glc} the HCA(CO)N experiment alone proved to be sufficient. An alternative assignment strategy, which utilizes several additional 3D triple-resonance NMR experiments together with the 3D HCCH-COSY and HCCH-TOCSY experiments (Ikura et al., 1990, 1991a), has recently been successfully applied to the ~40% homologous IIA^{glc} protein from *E. coli* (Pelton et al., 1991).

Empirical correlations between $^{13}C^{\alpha}$ chemical shifts and secondary structure have recently been reported for a small number of proteins in solution (Spera & Bax, 1991; Wishart et al., 1991). Both studies noted a downfield shift (3.1 and 2.3 ppm average, respectively) for $^{13}C^{\alpha}$s in helical conformations and an upfield shift (−1.5 and −1.3 ppm average, respectively) for $^{13}C^{\alpha}$s in β-strand or extended conformations. Figure 9 shows the secondary shift differences between the $^{13}C^{\alpha}$ chemical shifts of IIA^{glc} and the random-coil shifts (Richarz & Wüthrich, 1978) plotted versus the residue number. The location of β-strands I–XIII and regions of helical conformation, as identified in the 2.2-Å crystal structure of IIA^{glc} (Liao et al., 1991), are indicated at the top of the figure. The average shift for the β-sheet $^{13}C^{\alpha}$ resonances is −1.7 ppm, with a standard deviation of 1.6, which is consistent with the observations of Spera and Bax (1991) and of Wishart et al. (1991). The average shift for the $^{13}C^{\alpha}$ resonances from the reported helical regions of IIA^{glc} is 1.8 ppm, with a standard

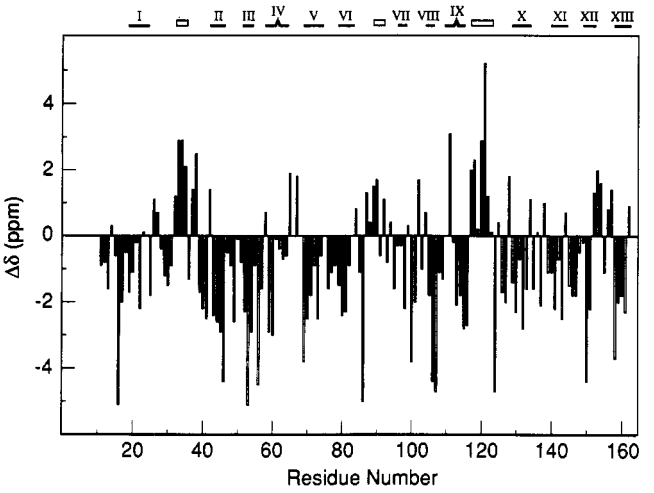

FIGURE 9: Plot of the differences between the $^{13}C^{\alpha}$ chemical shift and the random-coil shift (Richarz & Wüthrich, 1978) versus the residue number of IIA^{glc}. The locations of antiparallel β-strands I–XIII within the sequence are illustrated at the top. The peak in the lines for IV and IX represents a β-bulge. The regions 32–35, 89–91, and 117–123, defined as being in a helical conformation in the crystal structure (Liao et al., 1991), are indicated by open rectangles.

deviation of 1.4. The magnitude of this average downfield shift is lower than that observed previously for regions of regular helical structure (Spera & Bax, 1991; Wishart et al., 1991) and appears consistent with the earlier suggestion that, in solution, IIA^{glc} contains regions of irregular "helix-like" structure or helical turns only (Fairbrother et al., 1991). Similar conclusions were drawn from an analysis of the $^{13}C^{\alpha}$ chemical shifts of IIA^{glc} from *E. coli* (Pelton et al., 1991a).

Assignment of the side chain ^1H and ^{13}C resonances has proven essential in the determination of the solution structure of IIA^{glc}, because they allowed a number of side chain–side chain and side chain–backbone NOEs to be identified in the 3D ^1H–^{13}C NOESY-HSQC spectrum. The distance constraints thus obtained were critical for the determination of the solution structure because backbone distance constraints, alone, were insufficient to correctly calculate the fold of IIA^{glc} (Fairbrother et al., 1992). The resonance assignments obtained here, together with the backbone ^1H and ^{15}N assignments obtained previously (Fairbrother et al., 1991), will be necessary to obtain further distance constraints from 4D heteronuclear edited NOESY spectra (Kay et al. 1990c; Clore et al., 1991) in order to refine the current solution structure. In addition, they will allow the internal dynamics of IIA^{glc} to be investigated by measurement of ^{13}C and ^{15}N relaxation parameters (Stone et al., 1991) and should facilitate studies of the phosphorylated form of IIA^{glc} as well as studies of the HPr-IIA^{glc} complex.

ACKNOWLEDGMENTS

We are grateful to Dr. John Cavanagh for useful discussions and technical advice and to Mr. Timothy Burke for performing the N-terminal sequencing.

REFERENCES

Bax, A., & Subramanian, S. J. (1986) *J. Magn. Reson. 67*, 565–569.

Bax, A., Clore, G. M., Driscoll, P. C., Gronenborn, A. M., Ikura, M., & Kay, L. E. (1990a) *J. Magn. Reson. 87*, 620–627.

Bax, A., Clore, G. M., & Gronenborn, A. M. (1990b) *J. Magn. Reson. 88*, 425–431.

Bax, A., Ikura, M., Kay, L. E., & Guang, Z. (1991) *J. Magn. Reson. 91*, 174–178.

Clore, G. M., Bax, A., Driscoll, P. C., Wingfield, P. T., & Gronenborn, A. M. (1990) *Biochemistry 29*, 8172–8184.

Clore, G. M., Kay, L. E., Bax, A., & Gronenborn, A. M. (1991) *Biochemistry 30*, 12–18.

Dean, D. A., Reizer, J., Nikaido, H., & Saier, M. H., Jr. (1990) *J. Biol. Chem. 265*, 21005–21010.

Driscoll, P. C., Clore, G. M., Marion, D., Wingfield, P. T., & Gronenborn, A. M. (1990) *Biochemistry 29*, 3542–3556.

Fairbrother, W. J., Cavanagh, J., Dyson, H. J., Palmer, A. G., III, Sutrina, S. L., Reizer, J., Saier, M. H., Jr., & Wright, P. E. (1991) *Biochemistry 30*, 6896–6907.

Fairbrother, W. J., Gippert, G. P., Reizer, J., Saier, M. H., Jr., & Wright, P. E. (1992) *FEBS Lett. 296*, 148–152.

Fesik, S. W., Eaton, H. L., Olejniczak, E. T., Zuiderweg, E. R. P., McIntosh, L. P., & Dahlquist, F. W. (1990) *J. Am. Chem. Soc. 112*, 886–887.

Ikura, M., Kay, L. E., & Bax, A. (1990) *Biochemistry 29*, 4659–4667.

Ikura, M., Spera, S., Barbato, G., Kay, L. E., Krinks, M., & Bax, A. (1991a) *Biochemistry 30*, 9216–9228.

Ikura, M., Kay, L. E., & Bax, A. (1991b) *J. Biomol. NMR 1*, 229–304.

Kay, L. E., Ikura, M., & Bax, A. (1990a) *J. Am. Chem. Soc. 112*, 888–889.

Kay, L. E., Ikura, M., Tschudin, R., & Bax, A. (1990b) *J. Magn. Reson. 89*, 496–514.

Kay, L. E., Clore, M. G., Bax, A., & Gronenborn, A. M. (1990c) *Science 249*, 411–414.

Liao, D.-I., Kapadia, G., Reddy, P., Saier, M. H., Jr., Reizer, J., & Herzberg, O. (1991) *Biochemistry 30*, 9583–9594.

Live, D. H., Davis, D. G., Agosta, W. C., & Cowburn, D. (1984) *J. Am. Chem. Soc. 106*, 1939–1941.

Marion, D., Ikura, M., Tschudin, R., & Bax, A. (1989) *J. Magn. Reson. 85*, 393–399.

Palmer, A. G., III, Fairbrother, W. J., Cavanagh, J., Wright, P. E., & Rance, M. (1992) *J. Biomol. NMR 2*, 103–108.

Pelton, J. G., Torchia, D. A., Meadow, N. D., Wong, C.-Y., & Roseman, S. (1991a) *Biochemistry 30*, 10043–10057.

Pelton, J. G., Torchia, D. A., Meadow, N. D., Wong, C-Y., & Roseman, S. (1991b) *Proc. Natl. Acad. Sci. U.S.A. 88*, 3479–3483.

Powers, R., Gronenborn, A. M., Clore, G. M., & Bax, A. (1991) *J. Magn. Reson. 94*, 209–213.

Reizer, J., Saier, M. H., Jr. Deutscher, J., Grenier, F., Thompson, J., & Hengstenberg, W. (1988) *CRC Crit. Rev. Microbiol. 15*, 297–338.

Reizer, J., Sutrina, S. L., Wu, L.-F., Deutscher, J., Reddy, P., & Saier, M. H., Jr. (1992) *J. Biol. Chem.* (in press).

Richarz, R., & Wüthrich, K. (1978) *Biopolymers 17*, 2133–2141.

Saier, M. H., Jr. (1989) *Microbiol. Rev. 53*, 109–120.

Shaka, A. J., Barker, P. B., & Freeman, R. (1985) *J. Magn. Reson. 64*, 547–552.

Shaka, A. J., Lee, C. J., & Pines, A. (1988) *J. Magn. Reson. 77*, 274–293.

Spera, S., & Bax, A. (1991) *J. Am. Chem. Soc. 113*, 5490–5492.

Stone, M. J., Fairbrother, W. J., Palmer, A. G., III, Reizer, J., Saier, M. H., Jr., & Wright, P. E. (1992) *Biochemistry 31*, 4394–4406.

Sutrina, S. L., Reddy, P., Saier, M. H., Jr., & Reizer, J. (1990) *J. Biol. Chem. 265*, 18581–18589.

Wishart, D. S., Sykes, B. D., & Richards, F. M. (1991) *J. Mol. Biol. 222*, 311–333.

Wootton, J. C., & Drummond, M. H. (1989) *Protein Eng. 2*, 535–543.

Worthylake, D., Meadow, N. D., Roseman, S., Liao, D., Herzberg, O., & Remmington, S. J. (1991) *Proc. Natl. Acad. Sci. U.S.A. 88*, 10382–10386.